

A Review of Stratum-Drilling Robots: Developing for Seabed Exploration

AUTHORS

Peihao Zhang^{ID}

Ocean College, Zhejiang University

Jiawang Chen^{ID}

Ocean College, Zhejiang University
The Engineering Research Center of
Oceanic Sensing Technology and
Equipment, Ministry of Education,
Zhoushan, China

Zhenwei Tian

Hai Zhu

Ziqiang Ren^{ID}

Ocean College, Zhejiang University

ABSTRACT

This paper proposes a drilling robot solution for subsea stratum exploration and monitoring by analyzing the shortcomings of existing survey equipment in gas hydrate development. The current stratum-drilling robots applied to subsea environments are described in detail, including their development objectives, detection capabilities, structural components, research progress, and test results. Since several structural and functional similarities exist between planetary exploration and seabed stratum-drilling robots, and the development of planetary exploration-drilling robots is more sophisticated, various land-based stratum-drilling robots with characteristics are also summarized in detail. Finally, this paper summarizes, compares, and analyzes these stratum-drilling robots, including structure, motion modes, and test effects. Furthermore, this study develops evaluation criteria for stratum-drilling robots and provides effective research references and clear research directions for future development of seabed stratum-drilling robots.

Keywords: subsea environment, stratum-drilling robot, planetary exploration-drilling robot, gas hydrate

Introduction

Natural gas hydrates are ice-like caged compounds formed by water and hydrocarbon molecules under low temperature and high-pressure conditions (Chen & Wu, 2010; Fang et al., 2001). The total global reserves of natural gas hydrates are equivalent to about twice the total amount of proven conventional fossil energy (Wang et al., 2016). Thus, natural gas hydrates are expected to become the most abundant alternative energy source after shale gas, coalbed methane, and oil sands (Jiang et al., 2008). Natural gas hydrates are mainly contained in subsea sediments and terrestrial permafrost zones. According to statistics, hydrates are distributed in the Pacific Ocean, Indian Ocean, and polar regions, accounting for 1/4 of the total area of Earth's oceans, and are mainly concentrated in the seafloor from 500 to 2,000 m deep (Andresen & Huuse, 2011; Cartwright, 2011;

Cartwright et al., 2003; Sun et al., 2010). The greatest challenge in developing gas hydrates is discovering seafloor deposits and the geological changes encountered in the extraction process.

The most used geophysical exploration tools in gas hydrate explorations are seismic exploration, coring, and logging. Seismic exploration is mainly a preliminary investigation of the regional hydrate inventory, which is a reference for other subsequent geophysical explorations and drilling investigations. The coring technique provides the most intuitive and effective data on hydrate samples, but this method is costly. Logging technology can provide continuous high-resolution observation records of hydrate-bearing formations in the vicinity of log holes, providing an essential basis for understanding the in-

situ properties of subsea hydrates and their host sediments, estimating hydrate saturation, and predicting hydrate distribution, but it also requires the cooperation of subsea drilling rigs, which are still costly and difficult to operate, as well as difficult to achieve long-term mobile monitoring (W. Zhang et al., 2018; Zhong et al., 2020).

The emergence of stratum-drilling robotics can be an important tool for subsea gas hydrate or other resource investigation, which can well compensate for the limitations of the above-mentioned technology. The robot that enters the subsea stratum is released through the seabed base station. The sensors arranged on the robot body and the tail streamer can be used as new drilling and detection methods. The stratum-drilling robot can drill, penetrate, and steer through

the seabed stratum, and transmit the collected sediment stratigraphic information back to the seabed base station, which can act as both a release device for the robot and a relay for the subsea data signal and the sea surface-receiving vessel or device. Compared with coring, logging, and other methods of seabed sediment stratum detection, drilling robots, having sensors, can effectively improve the detection efficiency, which is convenient, efficient, economical, and will certainly be the trend of seabed sediment stratum detection, and even other applications of environmental stratigraphic detection in the future.

This study introduces the research progress of drilling robots applied to seabed stratigraphic environments. Due to the short development time of stratum-drilling robots for subsea applications, this paper also introduces the research progress of planetary exploration-drilling robots with similar structures and unmanned application scenarios as an important reference for the future design of seabed stratum-drilling robots. The next section introduces the structural composition, working principle, performance, and research progress of seabed-drilling robots. The following section dwells on the structural composition, working principle, performance, and research progress of planetary exploration-drilling robots. Furthermore, the next section compares and analyzes different stratum-drilling robots, mainly including size, structure, exploration target, power mechanism, test results, whether they can take samples or carry sensors, and other performance. Finally, the concluding section summarizes the current progress of stratum-drilling robots and the challenges in the future development process.

Seabed-Drilling Robots

This section focuses on the research of drilling robots applied in underwater environments, such as the seabed stratum. Depending on their application purpose, drilling robots used on the seabed can be broadly classified into oil and gas extraction, auxiliary work, and monitoring. Since the design purposes of seabed-drilling robots are different, their sizes also vary greatly. Also, this section introduces the seabed stratum-drilling robots mainly in terms of design purpose, target depth, function, size, working form, and structure.

Rigid Bionic Type of Drilling Robot

The Badger Explorer was proposed by Badger Explorer ASA of Norway in 1999 as a new drilling method that does not require an offshore drilling platform or rig. The main design purpose of the Badger Explorer is exploration in offshore oil and gas extraction. It relies on gravity for automated drilling and can measure engineering and strati-

graphic parameters in real time during drilling such as pore formation pressure, rupture pressure, temperature, porosity, permeability, and saturation, and stay at the bottom of the well for long-term monitoring of the reservoir after reaching the target depth.

The Badger drill has a 25-m body length, a 15-cm diameter, 10-kW power, and is designed to drill to a 3,000-m depth. From the tail-end to the front-end, the Badger Explorer comprises the following: (1) debris compression head, (2) separation system, (3) front anchor, (4) cable bin and release equipment, (5) power supply and controller, (6) logging unit, (7) telescoping unit controlled by drilling-pressure, (8) rear anchor, (9) debris crushing and transportation unit, (10) drill bit (Stokka, 2002, 2006). Figure 1 shows its structure.

For subsea oil and gas exploration, the Badger Explorer is launched to the seabed-drilling rig by the mother vessel and connected to a power supply base station adjacent to the drilling site by a remotely operated

FIGURE 1

Badger Explorer. (a) 2D engineering drawing. (b) parts of Badger Explorer prototype.

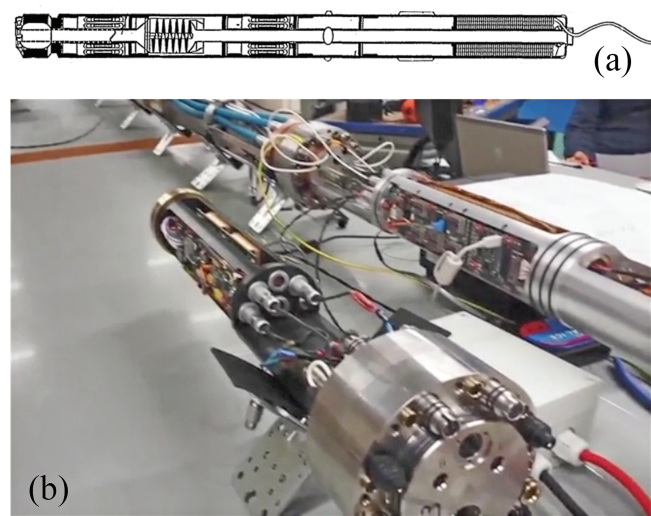
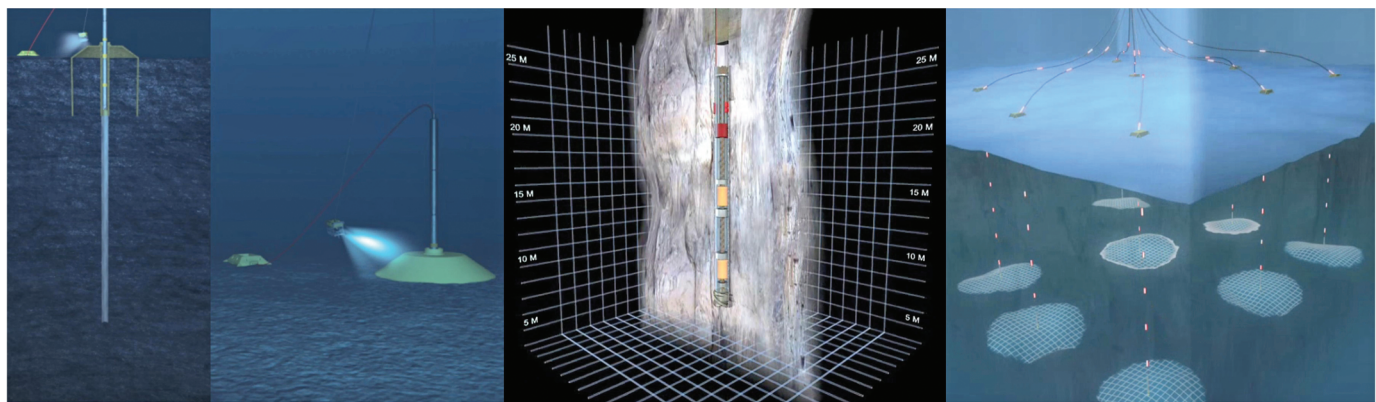


FIGURE 2

Schematic of Badger Explorer drilling process.



vehicle. After the power is turned on, the Badger Explorer drills forwards autonomously due to gravity without other propulsion. When the Badger Explorer operates, the front anchor grips the well wall, and the telescoping unit extends to drive the bit to drill. When the penetration length reaches the elongation limit of the piston, the rear anchor extends outward to grip the well wall, the front anchor contracts, and the telescoping unit retracts. Then, the telescoping unit regains its initial position, and a drilling process is completed. The Badger Explorer repeats these actions until the specified drilling depth is attained. The debris particles are then transported to the front part of the Badger Explorer, where they are compressed by the debris compression head into a dense debris plug and pushed out from the end. The drilling process is shown in Figure 2.

In 2007 and 2010, full-scale tests were conducted in a closed well, and the shallower depth of the Badger Explorer was achieved by piloting the borehole. Furthermore, in 2011, full-scale drilling and debris compression tests were conducted in a seabed-closed bare-hole section of

the Brumunddal Sandstone, a 234-m depth was drilled, and a 216-m debris column was compressed, showing good results (Guang et al., 2016).

Inspired by the Atlantic razor clam, Massachusetts Institute of Technology researchers developed a bionic digging robot, RoboClam. Based on the excellent digging performance of the Atlantic razor clam, RoboClam, which is compact, lightweight, and low-energy, developed a reversible and dynamic burrowing system for use in subsea ap-

plications, such as anchoring, oil exploitation, mineral extraction, and sensor placement (Winter et al., 2010).

The actuation system of the RoboClam comprises two nested pneumatic pistons (Figure 3a). The RoboClam is 9.9-cm long, 1.52-cm closed, and ~0.64 cm when it is open, the same size as the Atlantic razor clam (Winter et al., 2013, 2009). To make the neoprene boot shell evenly stressed during the opening process, the new generation RoboClam 2 adopts a three-sided

FIGURE 3

(a) RoboClam biomimetic burrowing robot and RoboClam actuation system. (b) Prototype of RoboClam 2.

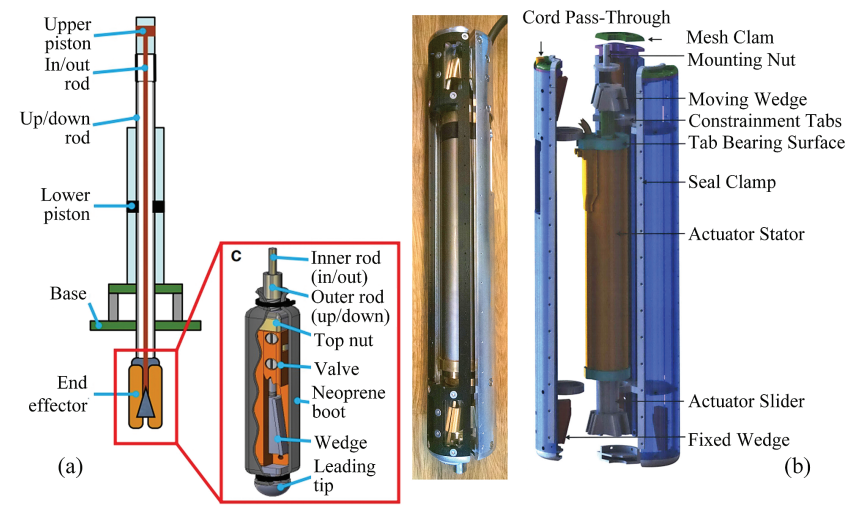
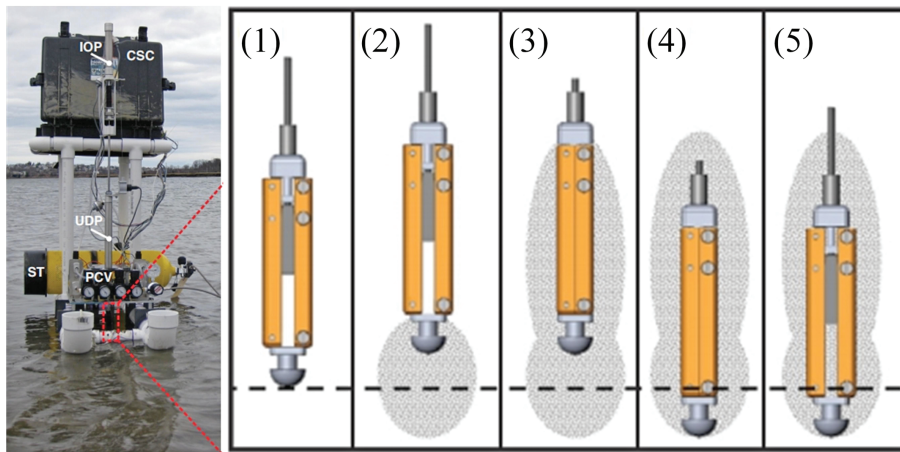


FIGURE 4

Motion process of RoboClam.



outward telescoping shell, and the external air drive is replaced by a built-in electric drive unit. The surface of the wedge block is coated with Teflon, which increases the mechanical efficiency to 55%, and it contracts at a maximum rate of 0.054 m/s (Dorsch & Winter, 2015; Isava & Winter, 2016). Its structure is shown in Figure 3b.

The motion process of the RoboClam is shown in Figure 4. The RoboClam starts in the opening state; when the air source in the driving system makes the up-down piston move, the robot moves upward, making the front soil fluidized. Then, the in-out piston moves and drives the wedge to make the neoprene boot contract.

The soil around RoboClam is fluidized, the resistance to robot movement is greatly reduced, and the robot moves downward rapidly by gravity (Winter et al., 2013). The RoboClam conducted functional tests on a substrate comprising soda-lime glass beads-simulated subsea soil (Winter & Hosoi, 2011; Winter et al., 2009). The RoboClam also conducted penetrating tests on an actual razor clam living environment, in which the robot control parameters were controlled by genetic algorithms for best optimization strategies (Isava & Winter, 2016; Winter et al., 2010; Winter et al., 2014). This result provides a basis for exploring the land applications of the RoboClam series (Isava & Winter, 2015).

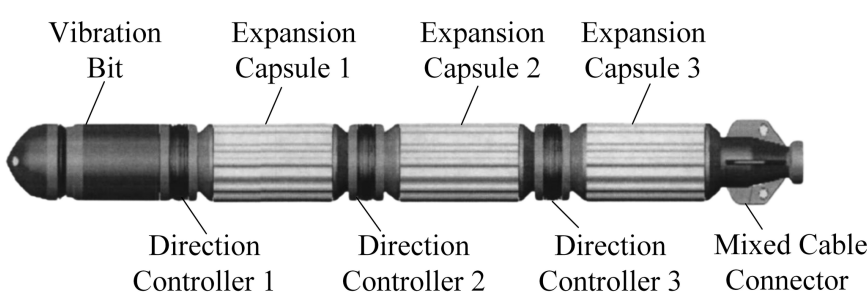
Capsule Bionic Type of Drilling Robot

The underwater bionic move-in-mud robot (UBMimR) is a robotic device used for shipwreck salvage near shore and at river mouths, which was developed by Wuhan University of Technology. It is designed to bind the wreck by carrying a lifting cable at the end of the robot that passes through the sediment on the lower side of the wreck. The UBMimR can replace divers to perform this hazardous task efficiently (Y. Zhang et al., 2005).

The UBMimR is designed with a linear structure, with a single body section (including the directional controller and expansion section) of ~800-mm length and a 3,500-mm total length, with a 225-mm diameter. From the head to the tail-end, there are a vibration bit, direction controller, main body section, and hybrid cable interface compartment in order, where the unit comprising the direction controller and the main body section is repeatedly arranged with three parts. The specific structure is shown in Figure 5. The UBMimR uses the hydraulic drive, and the interior of the vibration bit comprises the hydraulic vibrator and propulsion cylinder. The expansion capsule comprises two-layer parts. Driven by the hydraulic system, the inner capsule expands and contracts, and the outer capsule is superimposed with metal sheets forming a scale-like structure to prevent the inner capsule from being punctured (Y. Zhang, 2005). The direction controller comprises two cylinders mechanically interlocked into one group, and the two groups are arranged vertically, similar to a universal joint. The two pairs of interlocking cylinders can make the directional controller realize

FIGURE 5

Underwater bionic move-in-mud robot.



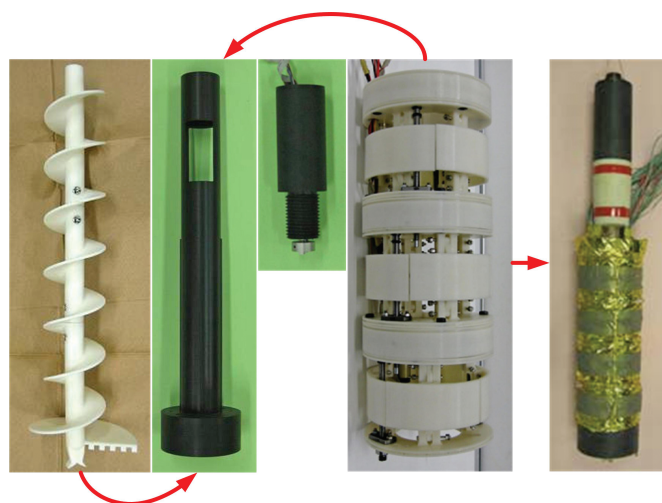
two steering degrees of freedom (DOFs).

With the goal of exploring and sampling superior planets to investigate the evolutionary history of the Earth and discover new resources, the Chuo University in Japan developed a planetary exploration robot based on a pipeline robot (Norihiko & Takashi, 2008; Omori et al., 2008, 2009). Due to the high similarity between the subsurface exploration of superior planets and the exploration of subsea sediment layers, and to improve the situation that conventional sediment exploration can only target one site for vertical excavation, researchers at Chuo University developed a seabed excavation robot based on the peristaltic crawling principle, which can also be used as a platform for various deep-sea observations and measurements (Nagai, Mizushina, Nakamura, Sugimoto, & Yoshida, 2015).

The planetary exploration robot comprises two parts: the propulsion and excavation mechanisms (Omori et al., 2011). The propulsion mechanism of the robot comprises three to four sections, and each propulsion section comprises belt drive and dual-pantograph mechanisms. When the motor drives the pulley and rotates the timing belt, the ball screw generates a contraction force, and under this movement, the dual-pantograph mechanism generates an axial drive force (Omori et al., 2013). The excavation mechanism comprises three parts: excavation, transport, and discharging. Its Earth auger is tapered using a fishtail single-auger-type blade, and a hem is installed on the auger to help transport the excavated soil smoothly. The transport section is a blade integrated with the auger (Kitamoto et al., 2013; Nagaoka,

FIGURE 6

Layout of excavation robot.



2011; Omori, 2014). The discharging unit comprises a bucket and a base part placed below the discharging port. The winder is erected above the robot to control the lifting of the bucket, which can be repeated for soil collection, handling, and discharge. The overall structure and layout of the robot is shown in Figure 6.

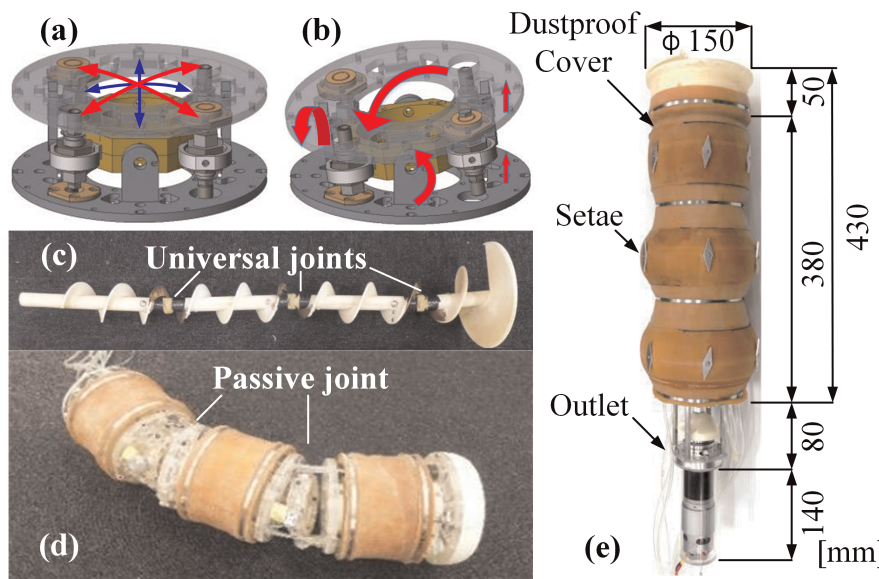
In the design of the seabed robot, the original motor-driven dual-pantograph mechanism is replaced by a hydraulically driven artificial muscle, which enables withstanding the high pressure of the subsea environment in the propulsion mechanism design (Nagai, Mizushina, Nakamura, Sugimoto, Watari, et al., 2015). Besides, the anti-rotation bristles are added externally to enhance the torque of the robot in the soil (Tadami et al., 2019). To reduce the excavating resistance of the front end, a jet device is added to the drill bit, which can spray water inwardly at 45° to the drilling direction to fluidize the soil front (Isaka et al., 2018). Gimbaled joints are added to the soil-transporting auger rods to be bent passively with the external body sections. An active steering mechanism driven

by four miniature hydraulic cylinders is added between the propulsion sections so that the bending and steering of the robot can be precisely controlled (Nagai et al., 2016; Tadami et al., 2017). The structure is shown in Figures 7(a)–(d). After continuous updating and iteration, various robot structures are optimized, leading to the current SEAVO II seabed excavation robot (Isaka et al., 2019). It is shown in Figure 7(e).

The structures of UBMimR and SEAVO series have a high similarity; they all move in the peristaltic style. We use the SEAVO series as an example to introduce the motion principle of the capsule bionic type of drilling robot. Each propulsion section is labeled as Subunits 1, 2, and 3 starting from the earth auger. Figure 8 shows the following five steps. (1) Each sub-unit contacts with the hole wall. (2) Subunit 1 contracts and moves forward. (3) Subunit 1 expands again. Afterward, Subunit 2 contracts and moves forward. (4) Subunit 2 expands again. Then, Subunit 3 contracts. (5) Subunits 1 and 2 move backward simultaneously. The robot body moves

FIGURE 7

(a)–(d) Bending joint and bent state structures. (e) Dustproofed SEAVO II.



forward relative to the starting position. Such movement uses hydraulic thrust than gravity and does not require squeezing through the soil, which can greatly reduce the resistance (Isaka, Tsumura, Watanabe, Toyama, & Nakamura, 2020).

The UBMimR uses fuzzy control rules analysis for the robot bionic autonomic peristalsis and postural adjustment motion (Y. Zhang, 2007). But there are no results related to the prototype and sea trials of the UBMimR.

During the development of the SEAVO II robot, several tests were conducted to verify the effectiveness of each optimized component (Nagai, Mizushina, Nakamura, Sugimoto, & Yoshida, 2015; Nakatake et al., 2016). In the overall tests, SEAVO II excavated in dry soil and in a kaolin-simulated subsea soil with 60% water content (Figures 9a and 9b), achieved a 650-mm maximum excavating depth and a steering motion with a 1.67-m turning radius in the laboratory

(Isaka, Tsumura, Watanabe, Toyama, Okui, et al., 2020).

Land-Based Planetary Drilling Robots

Several structural similarities between planetary subsurface exploration and seabed-drilling robots can be used as important references for developing seabed-drilling robots. These planetary subsurface exploration drilling robots are used for detecting, sampling, and long-term monitoring of superior planets, such as Mars and Mercury, and the Moon. In this section, several types of planetary subsurface exploration robots are introduced in terms of structure, movement patterns, targets and depth, and sampling availability.

Spiral-Blade Type of Drilling Robot

To explore the lunar surface, such as burying scientific observation instruments like long-term seismometers, researchers at Japan Aerospace Exploration Agency (JAXA) developed an autonomous burrowing screw robot that can be released from large base stations on the surface and transport the removed soil backward (Nagaoka et al., 2008). The soil excavation function at the front-end of the robot relies on a conical logarithmic spiral drill bit. To resist the torque developed by the drill bit, the body is equipped with cylindrical spiral blades in opposite directions, and its structure is shown in Figure 10. When the robot is drilling, the drill bit excavates the soil, while the rear screw transports the soil backward, counteracts torsional torque, and provides the forward force (Nagaoka et al., 2009).

FIGURE 8

Locomotion method of SEAVO II.

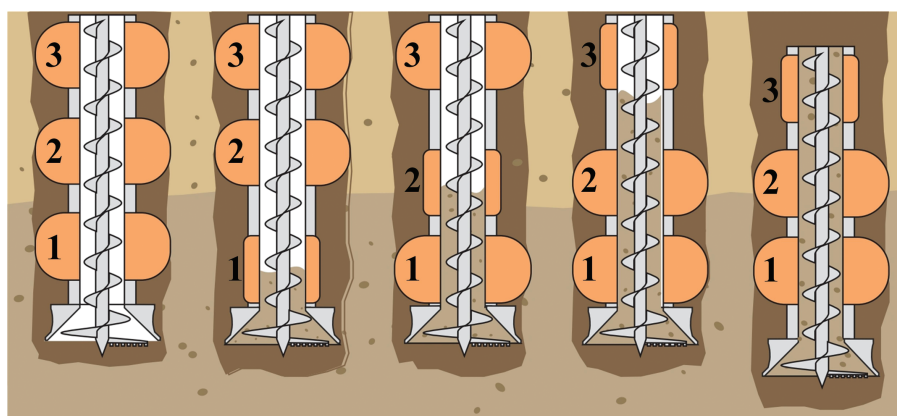


FIGURE 9

Excavation test results. (a) Bending excavation test. (b) Excavation test of SEAVO II in kaolin.



The researchers from JAXA developed another self-turning screw mechanism (STSM). The STSM mainly comprises the front and rear bodies, internal wheels, a motor (including clutch), a solenoid, an internal frame, and a dummy block of analog sensors. The exterior of the body is equipped with spiral blades. In the initial state, the clutch is separated, the front body is fixed, and the motor drives the wheels and the rear body to turn to dig the soil. When the clutch is connected, the rear body rotates with the front body. The motor is fixed with the inner frame, and the front body can rotate relative to each other. Meanwhile, the screw outside the body digs the soil, and the robot moves forward. Additionally, in Figure 11, Dummy A is a seismometer with a diameter and length of 50 mm,

respectively, and B is another simulated sensor. The structure of STSM is shown in Figure 11 (Yasuda, 2011).

Researchers at the University of Tsukuba in Japan developed the DigBot, a low-cost, convenient, and small excavation robot that uses a new drilling method called “contra-rotating drill.” There are two generations of DigBot prototypes, and they are composed of the drill bit and the propulsion mechanism. Prototype 1 uses a contra-rotating drill bit mechanism, which counteracts the torsional forces caused by drilling when digging into the excavated soil. The propulsion mechanism comprises eight solenoids arranged along a spiral line. When the robot is working, the eight solenoids are opened simultaneously; the propulsion of the robot relies on their

contact with the soil. Prototype 2 uses a simpler, plain, conical drill bit and a body composed of spiral blades. The cylindrical spiral blades on the body oppose the drill bit to provide the forward force, while counteracting the torque of the drill bit (Abe et al., 2010). The physical photograph of the two prototypes is shown in Figure 12.

Researchers from Carnegie Mellon University designed the Quad Digger, a robot that requires no release mechanism and can move on its own to a designated location and bury its body under the surface. This self-burying, dual-mode robot comprises four individual drill bits mounted at the corners of a rectangular frame, each of which can be rotated at 90°. The vertical and horizontal orientations of the drill bit indicate the drilling and moving modes, respectively. The interior of each drill bit contains a control panel and a drive device, and the exterior is the spiral blade. The spiral direction of each drill bit is opposite to an adjacent drill bit, so that the torque can be counteracted during drilling, ensuring that the robot does not require an additional holding fixture. The drilling direction of the robot changes by the differential control of the rotational speed of the four drill bits (Darukhanavala et al., 2013). Its two modes of motion are shown in Figure 13.

Researchers at the University of Ilmenau, Germany, developed an internally powered, low-cost, and efficient screw-driven autonomous drilling robot that can explore areas inaccessible to humans, such as superior planets, landslides, and reactor accident sites. The screw thread is the only major functional component of the robot, which serves to

FIGURE 10

Prototype of autonomous burrowing screw robot.

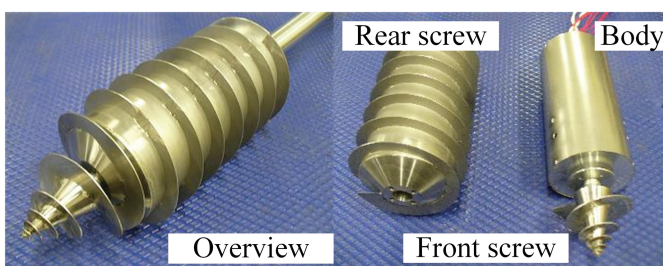
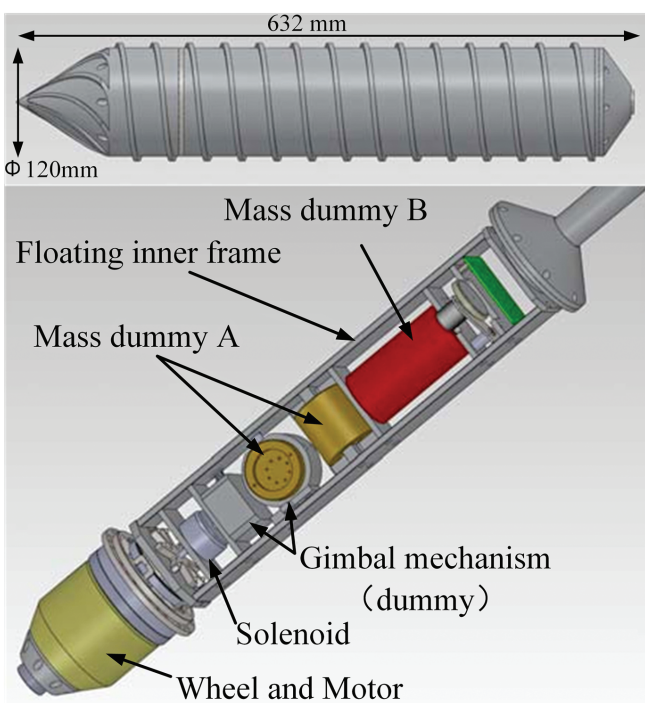


FIGURE 11

Overview and inner structure of STSM.



dig the soil at the front during the drilling process, while discharging the soil to the rear at an oblique angle to provide the forward force. The interior of the robot is installed with a battery, a motor, and other driving parts, and the exterior is equipped with antitorque panels. The maximum diameter of the screw-driven autonomous drilling robot is 28 mm, the width of the anti-torque panel is 81 mm, the total length is 204 mm, and the maximum

torque is 0.66 N (Becker et al., 2016). The exploded view of the screw-driven robot is shown in Figure 14.

The autonomous burrowing screw robot and STSM were tested several times in fly ash-simulated Martian and lunar soils. Results verify the actual motion effect of the robot. The STSM could penetrate to the bottom of the test setup (812.6 mm) after 24 h and 33 min and reversed the screw after reaching the bottom, it could also retreat most of the robot body

from the fly ash after 32 h and 42 min (Nagaoka et al., 2009). The test process is shown in Figure 15.

The Digbot Prototype 1 was tested in polypropylene pellets, and achieved a 38-mm maximum-drilling depth (Abe et al., 2010). The Quad Digger was tested in sugar, sand, and rice, materials of different densities, and particle sizes, to verify the drilling ability, and also tested in the motion mode to verify its motion function on a lawn (Darukhanavala et al., 2013). The screw-driven robot was tested in quartz sand, coarse-grained gravelly lava sands, and extremely fine cohesive chalky soil. It was demonstrated that the robot has a 200-mm maximum-drilling depth, a 4.6-mm/s drilling speed, and could work for 57 min with an 800-mAh battery (Lichtenheldt et al., 2017).

Bionic Type of Drilling Robot

The Inchworm deep drilling system (IDDS) was developed by National Aeronautics and Space Administration to carry sensors into planetary subsurfaces for exploration and sampling. It is divided into two drilling sections: descent and ascent sections. The descent section includes the radioisotope thermo-electric generator, whereas the ascent section has the linear actuator for axial telescoping and the sampler. Besides, both sections include the drill bit, drill motor, and supporting shoes. It uses the Sterling power system for energy supply, consumes less energy, and needs no connection by umbilical cords or ropes (Gorevan et al., 2003). The structure of IDDS is shown in Figure 16.

Researchers at the Harbin Institute of Technology, China, proposed a novel Inchworm Boring Robot (IBR). The IBR comprises three modules: drilling, propulsion, and discharging modules. The propulsion

FIGURE 12

Prototypes 1 (up) and 2 (down) of DigBot.

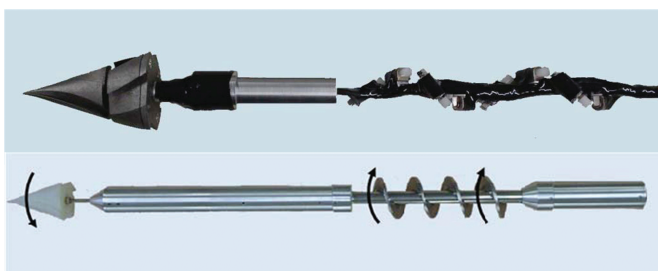


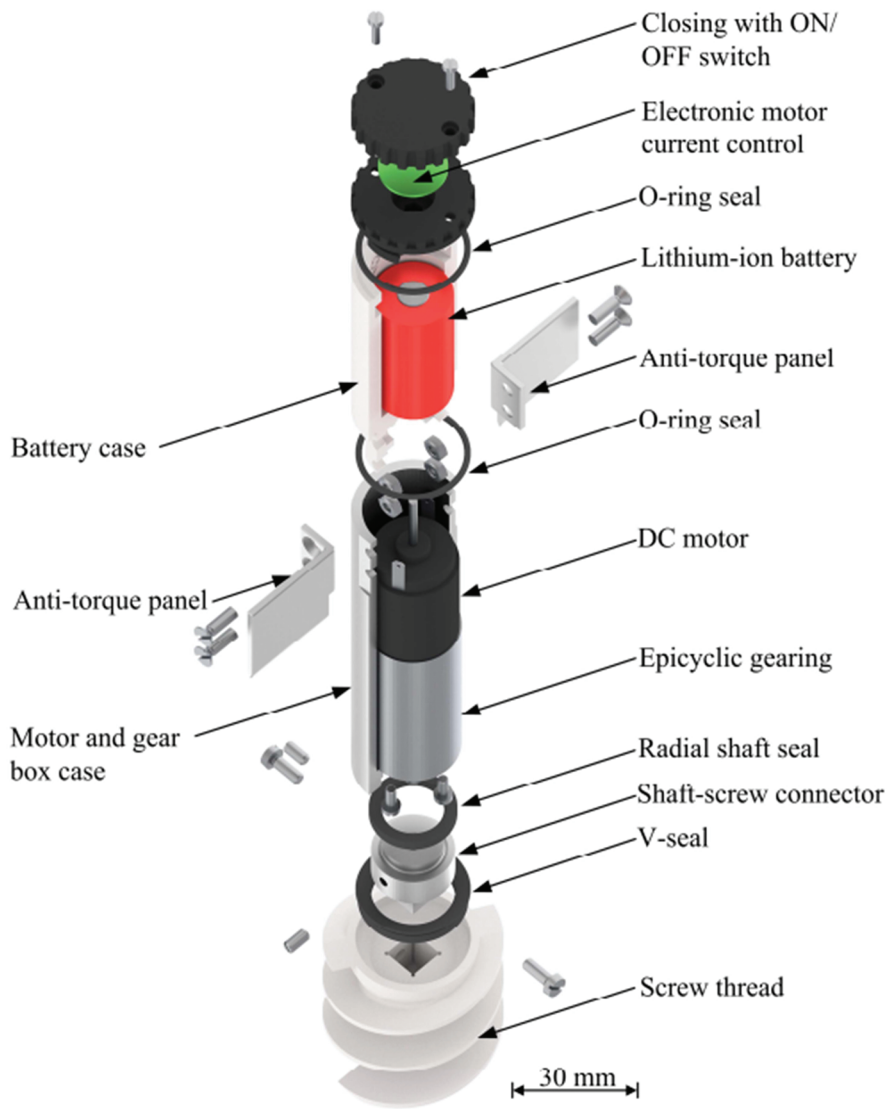
FIGURE 13

Quad Digger in two modes (Darukhanavala et al., 2013).



FIGURE 14

Exploded view of screw-driven robot prototype.



module moves inline between the drilling and discharging modules. The drilling module comprises a drill bit, auger-A, and anchor-A. Drill and auger-A break the raw rock into debris and transport the debris to the storage space. Auger-B in the discharging module can transport soil debris from the storage space to the back end. The drilling and discharging modules can be fixed on the borehole wall by Anchors A and B. When one of these two modules is fixed on the borehole wall, the other module is pulled or pushed forward by the propulsion module. The IBR was designed with a length of 500 mm, a diameter of 80 mm, a drill bit rotational speed of 94 rpm, and a total power of 90 W (Tang et al., 2015; W. Zhang et al., 2016, 2017). Its structure is shown in Figure 17.

The IDDS and IBR both adopt a pattern of movement imitating the inchworm. Several drilling tests of IBR were conducted using brown volcanic ash and Cenozoic alkaline olive basalt as simulants of the planetary surface soil. The robot could achieve a speed of 0.26 mm/s into the simulative regolith above 510 mm (Thomas & Stephen, 2006).

Researchers at the Korea Advanced Institute of Science and Technology designed a mole bot, a mole-like drilling robot, which is an embedded drilling system adopting the patterns of the incisor-using moles. This drilling robot uses a novel approach that requires no additional mechanism to discharge the soil (Kim et al., 2018). The most critical parts of the robot are the expandable drill bit and the forelimb soil-removing mechanism. The expandable drill bit of the mole bot is a new retractable mechanism that can be driven by a small actuator.

FIGURE 15

Test process of STSM.

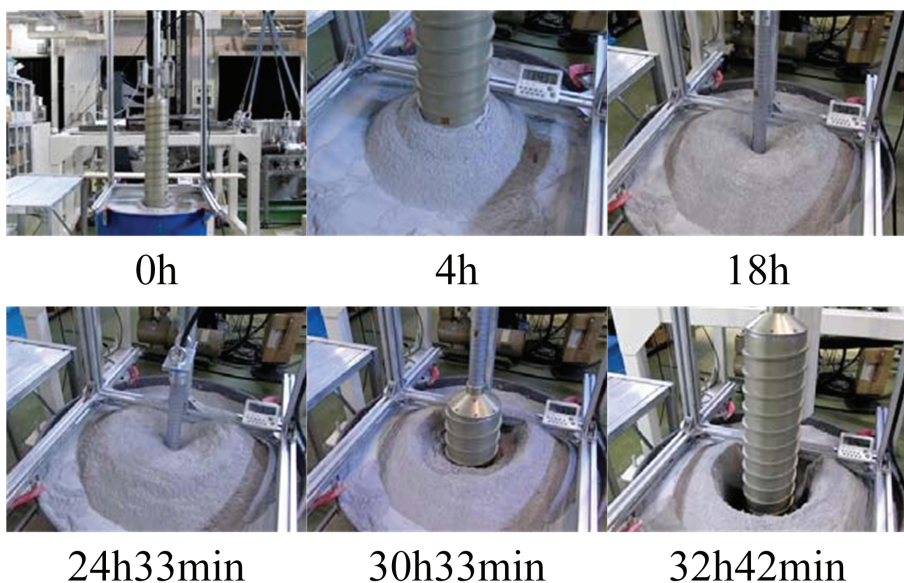
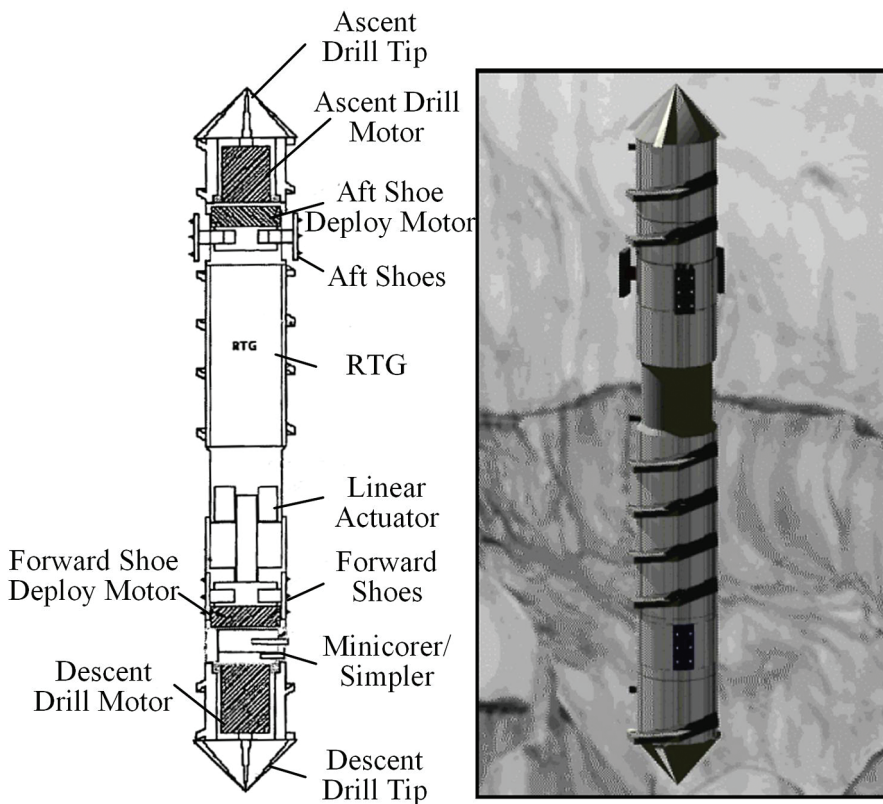


FIGURE 16

IDDS structure.



The expandable drill bit comprises three parts: the inner shaft, the middle part, and the outer casing. The blades that contact directly with the ground are classified as inner and expandable blades. Each expandable blade has a gear-shaped segment, which is connected with a rack and expands/folds at 90° by upward and downward motions. The drill bit expands when the motor rotates counterclockwise and folds in the opposite direction. The system can drill 93.4 and 202 mm in diameter in the folded and expanded states, with an expandability of 2.16 times the folded state (Lee et al., 2019). The forelimb soil-removing mechanism is part of the main body of the robot, and its action part comprises a bionic scapula and a front claw. The extension and retraction of the forelimb soil-removing mechanism are achieved by servo motors and two linear actuators. The linear speed difference of the scapula and front jaw is used to adjust the joint rotation, which enables the soil excavation and removal (Lee, Kim, & Myung, 2020; Lee et al., 2019). The structure of the mole bot is shown in Figure 18.

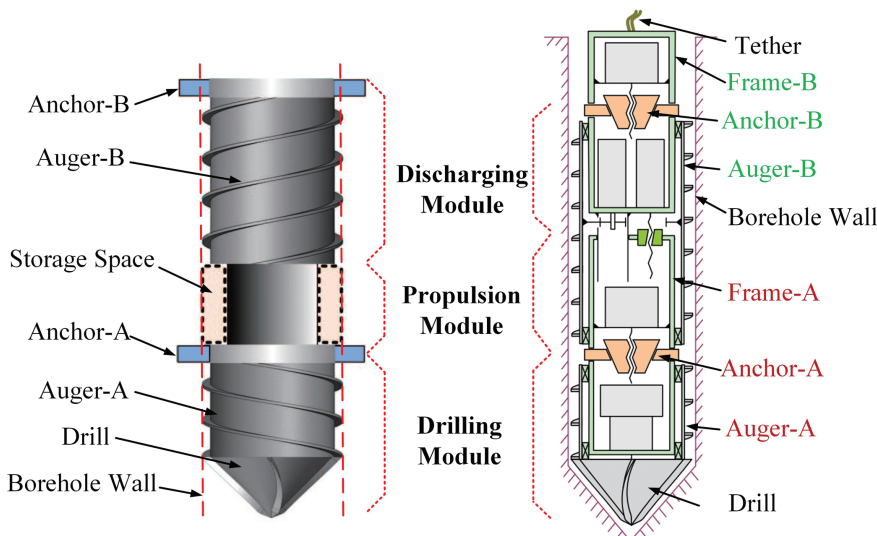
The researchers manufactured prototypes of the drill bit and the robot body to verify its drilling effectiveness and positioning method for moving in the soil. The optimal rate of penetration of the proposed mole bot was ~1.05 m/hr, which exceeds that of the existing drilling systems (less than 1 m hr), when the weight on bit was 93.3 N and the rotational speed was 124.49 rev/min. Figure 19 shows the digging sequence of the mole bot (Lee, Tirtawardhana, & Myung, 2020).

Other Types of Drilling Robots

The Moon Mars underground mole (MMUM) was built with support from

FIGURE 17

IBR structure.



the Mars Instrument Development Program to build a small, low-mass subsurface sampling system. With a 2-kg total weight, a 4-cm diameter, a 60-cm total length, and a 2-m maximum-drilling depth, the MMUM can collect 7-g soil samples, analyze the minerals using Raman spectroscopy, and measure its temperature. The front of the robot is the hammering mechanism, which comprises a drive unit and a striking mass. The soil temperature sensors and samplers are also arranged in the hammering head at the front-end. Attached to the back

of the hammering mechanism is a damping device, which avoids the reaction force applied to the instrument at the back, and is also an important part of the robot's ability to move through the soil. A Raman spectrometer is also arranged near the tail-end, and the optical head of the spectrometer is connected to the base station via a tail-end fiber. The MMUM structure is shown in Figure 20(a) (Stoker et al., 2007, 2003).

Researchers from Northeastern University developed the robotic planetary drilling system (RPDS).

The RPDS comprises a drill bit, a rotary propulsion unit, a power control module, a communication module, and a nonrotary steering unit, and it is powered by a Direct Current (DC) motor. The rotating propulsion and nonrotating steering units include three 3-DOF propulsion and three 1-DOF steering actuators, respectively. The three 3-DOF actuators are evenly distributed around the rotary propulsion unit, so that the drill bit rotates and moves forward in line, while the other three 1-DOF steering actuators provide the steering force (Liu et al., 2006a, 2006b).

Analysis and Comparison of Drilling Robots Application Scenarios

Both subsea- and land-drilling robots are used in extreme environments that are difficult to reach directly or unbearable for humans. There are three main application scenarios for subsea-drilling robots, including subsea resources and geological surveys, subsea oil and gas exploitations, and other types of subsea operations. Also, there are four application scenarios for land-drilling robots, including lunar and planetary exploration, surface soil sampling, improving prospecting efficiency, and military reconnaissance. It can be summarized that the main application scenario of both underwater- and land-drilling robots remains to detect the geological information of the soil, including the temperature, the ingredient, and the existence of other resources in it. The IDDS, MMUM, and RPDS can explicitly sample soils, but since all three robots are designed for planetary explorations, their functional implementation is more challenging, and

FIGURE 18

Structure of mole bot digging system.

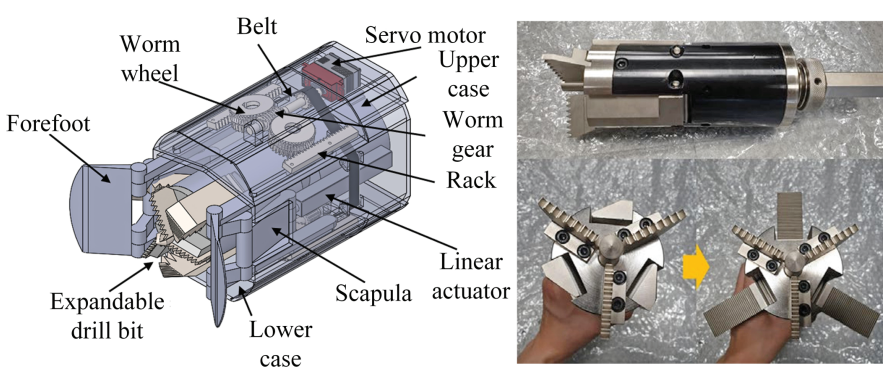
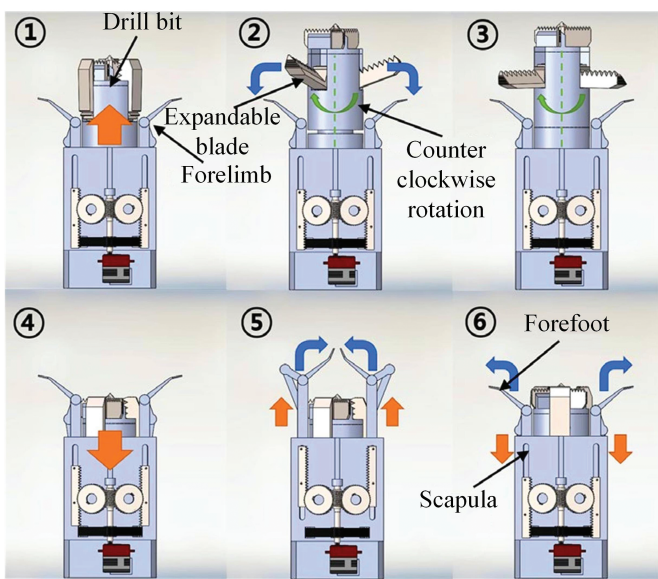


FIGURE 19

Digging sequence schematic of mole bot.



neither the IDDS nor the RPDS has a physical prototype. The underwater environment is more accessible than planets and other extreme environments, so underwater robots have more operational applications in addition to detection. Also, because the size of the carrier is almost unstinted in the marine environment, the size

and weight of the robot are less limited. Note that this less limited size of underwater-drilling robots is only comparable to land-drilling robots for planetary explorations. Because once it involves sampling the seabed stratum, the current research requires pressure maintaining of the sample. If the underwater robot has this function, its

size will increase significantly compared to only the detection function. Land-drilling robots are designed to carry sensors into the stratum for exploration in planets, and their functions, such as military reconnaissance and prospecting, are also an extension of the stratigraphic exploration function. It places high requirements on land-drilling robots to reach planets and extreme working environments, and the implementation of other functions must be based on accomplishing this objective. This objective requires high reliability for the movement pattern and communication methods of the robot.

Structures of Robots

The structures of the stratum-drilling robots can be divided into four main sections: drill bit (excavating the soil), discharging (transporting the excavated soil), propulsion (moving forward), and supporting (anchoring into the hole) sections. We have summarized the robot structures in the sections on seabed-drilling robots and land-based planetary drilling robots, and the robot structures are classified in Table 1.

Table 1 concludes that not all robots have all four structures. For example, UBMimR and RoboClam have no discharging sections; ABSR and Digbot have one structure for soil discharging and robot propulsion, respectively; and the screw-driven robot's soil discharging and propulsion structures rely on the drill bit. When the drilled soil is the seabed sediment layer, it is soft and high in fluidity, so the excavation mechanism of the robot can be vibrational, and the discharging structure can be removed as well. Combining the discharging and propulsion structures or even having all three functions

FIGURE 20

(a) MMUM external and internal views with main components. (b) RPDS structure.

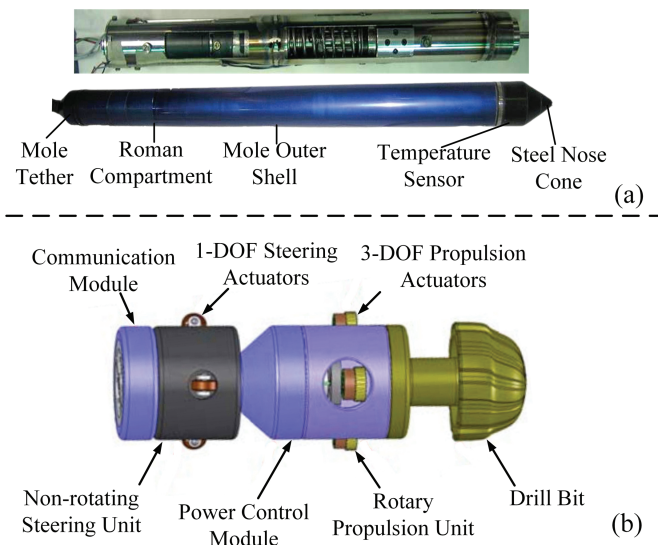


TABLE 1

Summary of structural components of various robots.

Name	Motion Structure			
	Drill bit	Discharging	Propulsion	Supporting
Badger Explorer	✓	✓	✓	✓
UBMimR	✓	✗	✗	✓
RoboClam	✗	✗	✗	✓
SEAVO	✓	✓	✗	✓
ABSR	✓	✗	✓	✗
STSM	✓	✗	✓	✗
Digbot	✓	✗	✓	✗
Quard Digger	✓	✗	✓	✗
Screw-driven robot	✓	✗	✗	✗
IDDS	✓	✓	✓	✓
IBR	✓	✓	✓	✓
Mole-like drilling robot	✓	✓	✓	✓
MMUM	✓	✗	✗	✗
RPDS	✓	✗	✓	✗

Note. ✓ means that the robot has this structure; ✗ means the robot does not have this structure.

performed by the drill bit can minimize the complexity of the structures and movement steps, which is important for applications with strict requirements for load weight and running time.

The drill bit structure of the stratum-drilling robot is divided into traditional rock and spiral blade bits. The traditional rock bit depends on the internal transport structure to discharge or transfer the soil debris. The novel spiral blade bits, which have logarithmic or cylindrical spiral blades outside the conical core column, can break up the soil directly and squeeze it toward the borehole wall from the rear. For example, the drill bit of the screw-driven robot can provide forward power by squeezing the soil debris to the side and rear. The three main propulsion methods include support-telescoping-type, spiral blade-type, and wheel-type, as well as relying on

self-weight. The wheel propulsion structure is more demanding on the borehole because it should ensure there is a solid running plane for the wheel. Thus, it is only suitable for dry and shaped soil. The support-telescoping propulsion structure is highly applicable, as it can adapt to different soil environments by the changing support mechanisms. For example, UBMimR and SEAVO can support the borehole wall in the seabed sediment layer by hydraulic oil naan covered with bristles, whereas IDDS and IBR support the smooth borehole wall in fly ash with support feet.

In addition to the above structures, two of the stratum-drilling robots introduced in the Seabed-Drilling Robot section have a steering mechanism. The presence of this feature indicates that the length and diameter of the robot cannot be too large; a

large dimension increases the steering radius of the robot and the torsional force, which significantly increases the structural complexity of the robot and further increases the robot size. Also, when the penetration depths of most application scenarios are not large, there is no strong demand for the steering structure for the robots, especially planetary exploration robots.

The driving device is the most important part of the internal structure. The driving devices are mainly motors, and some of them use hydraulics to drive the supporting structure because some robots adopt a bionic earthworm-like peristaltic form, with a hydraulic source driving artificial muscle to support the borehole. Hence, the motor drive is more advantageous than the hydraulic drive, whether considering only the size of the robot body or the needed additional base stations build. However, the use of hydraulics as the drive structure is advantageous because it eliminates using pressure-resistant seals. Besides, the hydraulic drive also provides the robot with greater borehole wall support forces. For example, the torsional resistance force of a planetary exploration robot, which has a similar diameter with SEAVO II and uses ABS rigid plates as supporting feet, is 200 N. In contrast, the SEAVO II artificial muscle of a single body section can provide the same frictional force under 30-kPa air pressure, and its torsional resistance force will far exceed this value if it adopts the hydraulic drive (Isaka, Tsumura, Watanabe, Toyama, Okui, et al., 2020; Kitamoto et al., 2013). Hydraulically driven artificial muscles or oil capsules are in closer contact with the soil, and their resistance to torsion and support will be better.

Test Results

To ensure that the robot drilling and penetration results are closest to the actual working conditions during laboratory tests, most robots used quartz sand and fly ash as experimental materials for simulating soil drilling. The density, friction angle, cohesion, and particle size of these materials are close to those of planetary regolith, and the water absorption is poor and difficult to consolidate, making them high-quality surface soil simulants (Lichtenheldt et al., 2014). The underwater robot also used water-saturated sand and kaolin to simulate the drilling process in the seabed sediment, and the test data showed a different resisting torque than the dry soil test, which is necessary for developing the underwater robot.

In the drilling test, most of the robot's penetration depth is within 1 m,

ranging from 140 to 932 mm. The Badger Explorer was tested in a real seabed environment to a drilling depth of 237 m, whereas the other robots were tested in a laboratory or an imitated natural environment, which basically could not reach the designed depth. To study the drilling effect of the robots, Table 2 shows the ratio of the penetration speed to the body length and the penetration depth to the body length. When the depth-length ratio exceeds 1, the robot can penetrate all of its body below the stratum surface, which verifies the excellent penetration ability of the robot. The depth-length ratios of SEAVO, STSM, and IBR all exceed 1. However, their current penetration depths are not their depth limits due to the maximum depth limitation of the testing setup.

In addition to the depth-length ratio, the robot penetration speed and speed-length ratio are also critical.

The penetration speed of the robots under the test conditions of the simulated soil showed a large variation, with a minimum STSM speed of 0.48 mm/min. Furthermore, the maximum speed of the RoboClam series is 480 mm/min. The range of the speed-length ratio is also large, from 0.05 to 195.16. Whether the robot is clamped by the setup-supporting frame during the test and depth of the simulated soil affects the penetration speed of the robot, and to improve the energy efficiency of the drilling process, the speeds listed in Table 2 are not all the maximum penetration speeds of the robots. After analyzing all drilling robot tests, it can be concluded that robots with an average penetration speed exceeding 5 mm/min and a speed-length ratio exceeding 0.5 are more valuable in practical applications.

In addition to the reasons mentioned above, the large speed difference of the robots can also be caused by the motion principles of robots. The speed-length ratios of the RoboClam, DigBot, Quard Digger, and Screw-driven robots all exceed 60, indicating that all these robots can complete a body-length penetration depth within 1 hr without considering the maximum setup depth. The introduction in the sections on seabed-drilling robots and land-based planetary drilling robots highlighted that the motion principles of robots could be broadly classified into four types: fluidization-type, hammering-type, nonretroaction spiral-type, and supporting-peristalsis-type. DigBot, Quard Digger, and screw-driven robot belong to the nonretroaction spiral-type, whereas the robots with slower penetration speed and speed-length ratio belong to the supporting-peristalsis-type. The penetration

TABLE 2

Body length, penetration speed, and speed-length and depth-length ratios of robots.

	Length (mm)	Speed (mm/min)	Speed-length ratio	Depth-length ratio
Badger Explorer	25000	*	*	9.48
UBMimR	3500	*	*	*
RoboClam	384	480	75.00	0.84
SEAVO	650	138	12.74	1.44
ABSR	290	50	10.34	0.41
STSM	632	0.48	0.05	1.29
Digbot	300	300	60.00	1.27
Quard Digger	190	618	195.16	0.73
Screw-driven Robot	204	276	81.18	0.98
IDDS	2000	*	*	*
IBR	500	8.3	1.00	1.7
Mole-like Drilling Robot	360	17.5	2.92	0.65
MMUM	600	1.16	0.12	0.83
RPDS	500	5	0.60	*

Note. * means that this parameter is not available temporarily.

depth of the fluidization or hammering types is limited. It is difficult to overcome this limitation in principle, and it is difficult to achieve steering. The nonretroaction spiral-type has a considerable penetration speed. Although the penetration speed of the supporting-peristalsis-type is relatively low, it is more reliable in motion and can realize abundant motion functions (Appendix).

Summary and Outlook

The robots presented herein are robots with certain research progress and further research value; they are representative and unique in structural design and experimental effects. It can be concluded that robot designs are quite different for different applications, such as exploration and engineering operations. The design penetration depth of underwater-drilling robots is generally several times the robot length, and the penetration of planetary-drilling robots is mainly at the stratum surface due to the limitations of current aerospace technologies. The planetary robots focus on surface detection and sampling, and the underwater-drilling robots should realize more complex functions. When the penetration depth is small, the basic parameters, such as temperature and pressure, can be obtained using the sensor equipped in the robot body. However, when the penetration depth is large, the robot mainly drills, and the sensors can be placed in the borehole by carrying them on the back end of the robot.

Several differences exist in the size, drive-type, and motion modes of the robot. Due to the subdivision of application scenarios, and since most of the scenarios are currently

difficult to be tested in real conditions, it is not yet possible to form a unified stratum-drilling robot design standard to guide research works. However, in seabed stratum drilling, especially in resource exploration and development similar to the subsea natural gas hydrate sediment stratigraphy, robots like the SEAVO series from Chuo University in Japan have shown superior research contents and laboratory test results.

In the future design of stratum-drilling robots for seabed applications, the supporting-peristalsis type should become the most mainstream motion mode, whereas the active steering mechanism should also be an important part, which can extend the range of motion of the robot and ensure the controllability of the motion rhythm. Using hydraulic components for driving is more advantageous, avoiding the additional volume caused by the seal. Future research efforts should focus on new drill bits, with new structures that reduce the front-end resistance, remove penetration resistance from the borehole wall, and even provide forward momentum. Supporting sections with hydraulically driven artificial muscles will be more flexible and adaptable, whereas if rigid support feet are used, seals will need to be solved to ensure that mud does not get stuck during contraction and extension. In future design studies, the study of the positioning of the robot in the stratum and the development of the motion control software will also be considered. Furthermore, the seabed releasing base station will be included when developing the whole equipment.

From a holistic point of view, in the future development of subsea stratum-drilling robots, motor-driven and hydraulic-driven may become two technical routes. They may be applied in miniaturized, clustered op-

eration within shallow stratum, or heavy-duty, large-depth operations, respectively. With the development of the body structure and the software of the control systems, and the development of the supporting base station, the seabed stratum-drilling robot system will be significantly important in the exploration and exploitation of the seabed.

Corresponding Author:

Jiawang Chen
Ocean College, Zhejiang University and
The Engineering Research Center of Oceanic Sensing Technology and Equipment, Ministry of Education, Zhoushan, 31621, China
Email: arwang@zju.edu.cn

Acknowledgments

This work was supported by the National Natural Science Foundation of China (41976055), Key Special Project for Introduced Talents Team of Southern Marine Science and Engineering Guangdong Laboratory (Guangzhou; GML2019ZD0506), Fundamental Research Funds for the Central Universities (2019XZZX003-05), and Finance Science and Technology Project of Hainan Province (ZDKJ202019).

References

- Abe, R., Kawamura, Y., Kamijima, K., & Murakami, K. 2010. Performance evaluation of contra-rotating drill for DIGBOT. In: SICE Annual Conference 2010. pp. 885–8. Taipei, Taiwan: IEEE.
- Andresen, K., & Huuse, B. 2011. ‘Bulls-eye’ pockmarks and polygonal faulting in the Lower Congo Basin: Relative timing and implications for fluid expulsion during shallow

- burial. *Mar Geol.* 279(1–4):111–27. <https://doi.org/10.1016/j.margeo.2010.10.016>.
- Becker**, F., Börner, S., Lichtenheldt, R., & Zimmermann, K. 2016. Enabling autonomous locomotion into sand—A mobile and modular drilling robot. In: *ISR 2016: 47st International Symposium on Robotics*. Munich, Germany: VDE.
- Cartwright**, J. 2011. Diagenetically induced shear failure of fine-grained sediments and the development of polygonal fault systems. *Mar Petrol Geol.* 28(9):1593–610. <https://doi.org/10.1016/j.marpetgeo.2011.06.004>.
- Cartwright**, J., James, D., & Bolton, A. 2003. The genesis of polygonal fault systems: A review. *Geol Soc Lond Spec Pub.* 216(1): 223–43. <https://doi.org/10.1144/GSL.SP.2003.216.01.15>.
- Chen**, Z., & Wu, N. 2010. The current status of permafrost gas hydrate exploration and exploitation in the world and its implications (in Chinese). *Mar Geol Lett.* 26(11):36–44. <https://doi.org/10.16028/j.1009-2722.2010.11.008>.
- Darukhanavala**, C., Lycas, A., Mittal, A., & Suresh, A. 2013. Design of a bimodal self-burying robot. In: *2013 IEEE International Conference on Robotics and Automation*. pp. 5600–5. Karlsruhe, Germany: IEEE. <https://doi.org/10.1109/ICRA.2013.6631381>.
- Dorsch**, D., & Winter, A. 2015. Design of a Biologically Inspired Underwater Burrowing Robot That Utilizes Localized Fluidization. In: *ASME 2015 International Design Engineering Technical Conferences and Computers and Information in Engineering Conference*. Boston, MA: ASME. <https://doi.org/10.1115/DETC2015-47459>.
- Fang**, Y., Li, M., Jin, X., & Shentu, H. 2001. Character analysis of the marine gas hydrate stability zone (in Chinese). *Mar Geol & Quat Geol.* 21(1):4. <https://doi.org/10.16562/j.cnki.0256-1492.2001.01.018>.
- Gorevan**, S., Myrick, T., Batting, C., Mukherjee, S., Bartlett, P., & Wilson, J. 2003. Strategies for future mars exploration: An infrastructure for the near and longer-term future exploration of the subsurface of Mars. In: *6th International Conference on Mars. 6th International Conference on Mars: Pasadena, CA*. <https://www.lpi.usra.edu/meetings/sixthmars2003/pdf/3196.pdf>.
- Guang**, X., Wang, M., Huang, H., & Deng, H. 2016. Research progress and technology of Badger Explorer (in Chinese). *Drilling & Production Technol.* 39(6):4.
- Isaka**, K., Tadami, N., Fujiwara, A., Nakatake, T., Suzesawa, M., & Yamada, Y., ... Nakamura, T. 2018. Water jetting excavation and consideration of earth auger shape to reduce drilling torque for seabed robotic explorer. In: *2018 IEEE/ASME International Conference on Advanced Intelligent Mechatronics (AIM)*. pp. 887–92. Auckland, New Zealand: IEEE. <https://doi.org/10.1109/AIM.2018.8452688>.
- Isaka**, K., Tsumura, K., Watanabe, T., Toyama, W., & Nakamura, T. 2019. Development of underwater drilling robot based on earthworm locomotion. *IEEE Access.* 7:103127–41. <https://doi.org/10.1109/ACCESS.2019.2930994>.
- Isaka**, K., Tsumura, K., Watanabe, T., Toyama, W., & Nakamura, T. 2020. Soil discharging mechanism utilizing water jetting to improve excavation depth for seabed drilling explorer. *IEEE Access.* 8:2856028570. <https://doi.org/10.1109/ACCESS.2020.2972572>.
- Isaka**, K., Tsumura, T., Watanabe, T., Toyama, W., Okui, M., Yoshida, H., & Nakamura, T. 2020. Clay Drilling Performance of Seabed Robotic Explorer Using Peristaltic Motion. In: *2020 IEEE/SICE International Symposium on System Integration (SII)*. pp. 1340–7. Honolulu, HI: IEEE. <https://doi.org/10.1109/SII46433.2020.9026231>.
- Isava**, M., & Winter, A. 2015. Razor clam-inspired burrowing in dry soil. *Int J Nonlin Mech.* 81:30–9. <https://doi.org/10.1016/j.ijnonlinmec.2015.12.005>.
- Isava**, M., & Winter, A. 2016. An experimental investigation of digging via localized fluidization, tested with RoboClam: A robot inspired by Atlantic razor clams. *J Mech Design.* 138(12):125001. <https://doi.org/10.1115/1.4034218>.
- Jiang**, H., Qiao, W., Zhong, T., Song, X., Qi, R., & An, X. 2008. Status and forecast of world's natural gas hydrate exploration & development. *Sino-Global Energy.* 13:19–25.
- Kim**, J., Jang, H., Shin, J., Hong, J., & Myung, H. 2018. Development of a mole-like drilling robot system for shallow drilling. *IEEE Access.* 6:76454–63. <https://doi.org/10.1109/ACCESS.2018.2884495>.
- Kitamoto**, H., Omori, H., Nagai, H., Nakamura, T., Osumi, H., & Kubota, T. 2013. Propulsion mechanism for a lunar subterranean excavator using peristaltic crawling. *J Robot Mechatronics.* 25(3):466–75. <https://doi.org/10.20965/jrm.2013.p0466>.
- Lee**, J., Kim, J., & Myung, H. 2020. Design of Forelimbs and Digging Mechanism of Biomimetic Mole Robot for Directional Drilling. In: *6th International Conference on Robot Intelligence Technology and Applications*. pp. 341–51. Singapore: Springer. https://doi.org/10.1007/978-981-13-8323-6_28.
- Lee**, J., Tirtawardhana, C., Jang, H., Hong, J., & Myung, H. 2019. Concept design of a novel bio-inspired drilling system for shallow drilling. In: *2019 19th International Conference on Control, Automation and Systems (ICCAS)*. pp. 1276–80. Jeju, Korea (South): IEEE. <https://doi.org/10.23919/ICCAS47443.2019.8971518>.
- Lee**, J., Tirtawardhana, C., & Myung, H. 2020. Development and analysis of digging and soil removing mechanisms for mole-bot: Bio-inspired mole-like drilling robot. In: *2020 IEEE/RSJ International Conference on Intelligent Robots and Systems (IROS)*. pp. 7792–9. Las Vegas, NV: IEEE. <https://doi.org/10.1109/IROS45743.2020.9341230>.
- Lichtenheldt**, R., Becker, F., & Zimmermann, K. 2017. Screw-driven robot for locomotion into sand. In: *59th Ilmenau Scientific Colloquium. Die Digitale Bibliothek Thüringen: Ilmenau, Germany*. https://www.db-thueringen.de/servlets/MCRFileNodeServlet/dbt_derivate_00039324/ilm1-2017iwk-005.pdf.
- Lichtenheldt**, R., Schäfer, B., & Krömer, O. 2014. Hammering beneath the surface of Mars—Modeling and simulation of the impact-driven locomotion of the HP 3-Mole by coupling enhanced multi-body dynamics and discrete element method. In: *Shaping the future*

- by engineering: 58th Ilmenau Scientific Colloquium. Die Digitale Bibliothek Thüringen: Ilmenau, Germany. https://elib.dlr.de/90649/1/LichtenheldtSchaeferKroemer_full_paper_Proceedings.pdf.
- Liu, Y.**, Weinberg, B., & Mavroidis, C. 2006a. Design and modeling of the NU Smart Space Drilling System (SSDS). In: American Society of Civil Engineers 10th Biennial International Conference on Engineering, Construction, and Operations in Challenging Environments and Second NASA/ARO/ASCE Workshop on Granular Materials in Lunar and Martian Exploration. pp. 1–8. League City/Houston, TX: ASCE. [https://doi.org/10.1061/40830\(188\)96](https://doi.org/10.1061/40830(188)96).
- Liu, Y.**, Weinberg, B., & Mavroidis, C. 2006b. Mechanical design and modelling of a robotic planetary drilling system. In: ASME 2006 International Design Engineering Technical Conferences and Computers and Information in Engineering Conference. pp. 925–32. Philadelphia, PA: ASME. <https://doi.org/10.1115/DETC2006-99699>.
- Nagai, M.**, Hirabayashi, C., Yamada, Y., Nakamura, T., & Yoshida, H. 2016. Development of a flexible excavation unit for a peristaltic crawling seabed excavation robot. In: Advances in Cooperative Robotics, eds. Tokhi, M.O., & Virk, G.S., pp. 97–105. London, UK: World Scientific Press. https://doi.org/10.1142/9789813149137_0015.
- Nagai, M.**, Mizushina, A., Nakamura, T., Sugimoto, F., Watari, K., Nakajo, H., & Yoshida, H. 2015. Development of a hydraulic artificial muscle for a deep-seafloor excavation robot with a peristaltic crawling mechanism. In: ICIRA 2015: Intelligent Robotics and Applications. Cham, Switzerland: Springer, pp. 379–89. https://doi.org/10.1007/978-3-319-22879-2_35.
- Nagai, M.**, Mizushina, A., Nakamura, T., Sugimoto, F., & Yoshida, H. 2015. Development of seabed excavation robot with peristaltic crawling. In: 2015 IEEE/RSJ International Conference on Intelligent Robots and Systems (IROS). pp. 3869–74. Hamburg, Germany: IEEE. <https://doi.org/10.1109/IROS.2015.7353921>.
- Nagaoka, K.** 2011. Study on soil-screw interaction of exploration robot for surface and subsurface locomotion in soft terrain (Doctoral dissertation). Sokendai, Japan: Graduate University for Advanced Information. pp. 649–54. Shanghai, China: IEEE. <https://doi.org/10.1109/ICRA.2011.5979824>.
- Omori, H.**, Murakami, T., Nagai, H., Nakamura, T., & Kubota, T. 2013. Validation of the measuring condition for a planetary subsurface explorer robot that uses peristaltic crawling. In: 2013 IEEE Aerospace Conference. Big Sky, MT: IEEE. <https://doi.org/10.1109/AERO.2013.6496960>.
- Omori, H.**, Nakamura, T., & Takayuki, Y. 2009. An underground explorer robot based on peristaltic crawling of earthworms. Ind Robot. 36(4):358–64. <https://doi.org/10.1108/01439910910957129>.
- Stoker, C.**, Gonzales, A., & Zavaleta, J. 2007. Moon/Mars underground mole. https://www.academia.edu/7519883/Moon_Mars_Underground_Mole.
- Stoker, C.**, Richter, L., Smith, W., Lemke, L., Hammer, P., Dalton, J.B., ... Zent, A. 2003. The Mars Underground Mole (MUM): A subsurface penetration device with in situ infrared reflectance and raman spectroscopic sensing capability. In: 6th International Conference on Mars. <https://www.lpi.usra.edu/meetings/sixthmars2003/pdf/3007.pdf>.
- Stokka, S.** 2002. United States Patent No. WO/2002/014644.
- Stokka, S.** 2006. United States Patent No. 7093673.
- Sun, Q.**, Wu, S., Lue, F., & Yuan, S. 2010. Polygonal faults and their implications for hydrocarbon reservoirs in the southern Qiongdongnan Basin, South China Sea. J Asian Earth Sci. 39(5):470–9.
- Tadami, N.**, Isaka, K., Nakatake, T., Tujiwara, A., Yamada, Y., Nakamura, T., ... Yoshida, H. 2019. Underwater excavation by excavation robot equipped with propulsion unit based on earthworm setae. In: 2018 IEEE International Conference on Robotics and Biomimetics (ROBIO). pp. 51–8. Kuala Lumpur, Malaysia: IEEE. <https://doi.org/10.1109/ROBIO.2018.8664782>.
- Tadami, N.**, Nagai, M., Nakatake, T., Fujiwara, A., Yamada, Y., Nakamura, T., ... Kubota, T.

2017. Curved excavation by a sub-seafloor excavation robot. In: 2017 IEEE/RSJ International Conference on Intelligent Robots and Systems (IROS). pp. 4950–5. Vancouver, BC, Canada: IEEE. <https://doi.org/10.1109/IROS.2017.8206376>.
- Tang**, D., Zhang, W., Jiang, C., Shen, Y., & Chen, H. 2015. Development of an inch-worm boring robot(IBR) for planetary subsurface exploration. In: 2015 IEEE International Conference on Robotics and Biomimetics (ROBIO). pp. 2109–14. Zhuhai, China: IEEE. <https://doi.org/10.1109/ROBIO.2015.7419085>.
- Thomas**, M., & Stephen, G. 2006. United States Patent No. 7055625.
- Wang**, X., Hu, Y., Chang, Y., & Tang, J. 2016. Status and prospect of subsea natural gas hydrate exploitation technology. *Dev Energy Sci.* 4(1):5–13.
- Winter**, A., Deits, R., & Dorsch, D. 2013. Critical timescales for burrowing in undersea substrates via localized fluidization, demonstrated by roboclam: A robot inspired by atlantic razor clams. In: Asme 2013 International Design Engineering Technical Conferences & Computers & Information in Engineering Conference. Portland, OR: ASME. <https://doi.org/10.1115/DETC2013-12798>.
- Winter**, A., Deits, R., Dorsch, D., Hosoi, A., & Slocum, A. 2010. Teaching RoboClam to dig: The design, testing, and genetic algorithm optimization of a biomimetic robot. In: IEEE/RSJ International Conference on Intelligent Robots & Systems. pp. 4231–5. Taipei, Taiwan: IEEE. <https://doi.org/10.1109/IROS.2010.5654364>.
- Winter**, A., Deits, R., Dorsch, D., Slocum, A., & Hosoi, A. 2014. Razor clam to Robo-Clam: Burrowing drag reduction mechanisms and their robotic adaptation. *Bioinspir Biomim.* 9(3):036009. <https://doi.org/10.1088/1748-3182/9/3/036009>.
- Winter**, A., & Hosoi, A. 2011. Identification and evaluation of the Atlantic razor clam (*Ensis directus*) for biologically inspired subsea burrowing systems. *Integr Comp Biol.* 51(1): 151–7. <https://doi.org/10.1093/icb/icr038>.
- Winter**, A., Hosoi, A., & Slocum, A. 2013. United States Patent No. 8496410.
- Winter**, A., Hosoi, A., Slocum, A., & Deits, R. 2009. The design and testing of roboclam: A machine used to investigate and optimize razor clam-inspired burrowing mechanisms for engineering applications. In: ASME 2009 International Design Engineering Technical Conferences and Computers and Information in Engineering Conference. pp. 721–6. San Diego, CA: ASME. <https://doi.org/10.1115/DETC2009-86808>.
- Yasuda**, S. 2011. United States Patent No. 8061441.
- Zhang**, W., Jiang, S., Shen, Y., Li, P., & Chen, H. 2016. Development of an Inch-worm-type drilling test-bed for planetary subsurface exploration and preliminary experiments. In: 2016 IEEE International Conference on Robotics and Biomimetics (ROBIO), pp. 2187–91. Qingdao, China: IEEE. <https://doi.org/10.1109/ROBIO.2016.7866654>.
- Zhang**, W., Jiang, S., Tang, D., Chen, H., & Liang, J. 2017. Drilling load model of an inchworm boring robot for lunar subsurface exploration. *Int J Aerospace Eng.* 3:1–11. <https://doi.org/10.1155/2017/1282791>.
- Zhang**, W., Shao, M., Jiang, C., & Tian, Q. 2018. World progress of drilling and production test of natural gas hydrate. *Mar Geol Quat Geol.* 38(5):1–13. <https://doi.org/10.16562/j.cnki.0256-1492.2018.05.001>.
- Zhang**, Y. 2005. Research on underwater bionic move-in-mud robot and key technology (in Chinese; Doctoral dissertation). Wuhan University Of Technology.
- Zhang**, Y. 2007. Movement classifying and control for move-in-mud robot (in Chinese). *Ship & Ocean Eng.* 36(6):100–2.
- Zhang**, Y., Sun, H., Hu, Y., & Zhu, M. 2005. Research of underwater bionic move-in-mud robot (in Chinese). *J WUT (Inf Ma Eng).* 27(4):48–51.
- Zhong**, G., Zhang, D., & Zhao, L. 2020. Current states of well-logging evaluation of deep-sea gas hydrate-bearing sediments by international scientific ocean drilling (DSDP/ODP/IODP) programs (in Chinese). *Nat Gas Ind.* 40(8):25–44. <https://doi.org/10.1016/j.ngib.2020.08.001>.

Appendix
Summary of detailed robot parameters

TABLE A1

Summary of various robot structures and test parameters.

Type	Name	Monitor Model	Structure Parameters				Test parameters				Real World Testing	Research Level	
			Length (mm)	Diameter (mm)	Mass (kg)	Power (W)	Driving Form	Design Penetrating Deep (m)	Max Penetrating Deep (mm)	Penetrating Speed (mm/min)	Test Material		
Seabed drilling robot	Badger Explorer	Temperature/ Pressure/ Porosity	25 × 10 ³	150	*	10000	Electromotor	1500	237 × 10 ³	*	Sandstone	✓	Abundant
	UBMimR	x	3.5 × 10 ³	225	*	*	Hydraulic/ Electromotor	10	x	x	x	x	Normal
	RoboClam	x	384	56	3.6	*	Electromotor	*	323	480	Real beach	✓	Abundant
	SEAVO	x	650	150	31.5	*	Hydraulic/ Electromotor	10	938	138	Fly ash/ Toyoura sand/ Kaolin/ sand	✓	Abundant

continued

TABLE A1

Continued

Type	Name	Monitor Model	Structure Parameters			Test parameters			Real World Testing	Research Level	
			Length (mm)	Diameter (mm)	Power (W)	Driving Form	Max Penetrating Deep (m)	Penetrating Speed (mm/min)	Test Material		
Land-based drilling robot	ABSR	Seismometer	290	124	3.87	*	Electromotor	*	50	Fly ash/ Quartz sand	x
	STS M	Seismometer/ Heat flow sensor	632	120	11.6	100	Electromotor	*	812.6	Fly ash	x
	Digbot	x	300	50	*	*	Electromotor	1	380	Polypropylene pellet	x
	Quard Digger	x	270 × 270 × 190	75	5	100	Electromotor	*	140	618	✓
	Screw-driven Robot	x	204	28	0.15	*	Electromotor	400	200	276	Dry sand/rice/ sugar/flour
	IDDS	Temperature	2000	150	*	1000	Electromotor	100	*	Quartz sand/ Lava sand/ Chalk soil	x
	IBR	Temperature/ Chemical composition/ Mechanical property	500	80	3.5	50	Electromotor	*	850	8.3	Cenozoic alkaline olivine basalt
	Mole-like-drilling robot	x	360	202	7	*	Electromotor	*	233.31	17.5	Autoclaved lightweight concrete
MUM	Raman spectroscopy/ Temperature	600	40	2	10	Electromotor	2000	500	1.16	Dry sand/ Beach	x
	RPDS	x	500	150	50	570	Electromotor	*	5	*	Abundant
									*	normal	

Note. x means that there is no data; * means that this parameter is not available temporarily.